

Spectroscopic Study of the C  $^1\Sigma^+$  State of  $^6\text{LiH}$  and  $^7\text{LiD}$ 

Su-Kai Hsu, Jun-Jen Wang, Pyng Yu, Chia-Ying Wu, and Wei-Tzou Luh\*

Department of Chemistry, National Chung Hsing University, 250 Kuo-Kuang Road, Taichung 402, Taiwan

Received: January 8, 2002; In Final Form: April 11, 2002

The C  $^1\Sigma^+$  excited electronic state of  $^6\text{LiH}$  and  $^7\text{LiD}$  isotopomers has been studied by a pulsed optical–optical double resonance fluorescence depletion spectroscopic technique, in which a band-resolved laser-induced fluorescence detection scheme was used. Forty-two  $^6\text{LiH}$  vibrational ( $\nu = 2–43$ ) levels and fifty-five  $^7\text{LiD}$  vibrational ( $\nu = 4–58$ ) levels have been separately observed. The absolute vibrational numbering of the  $^7\text{LiD}$  C  $^1\Sigma^+$  state is identified via a comparison between observed term values and those calculated with a hybrid potential energy curve reported previously for the  $^7\text{LiH}$  C  $^1\Sigma^+$  state. Among the highest observed vibrational levels, the highest observed rovibrational levels are respectively the (43,5) level for  $^6\text{LiH}$  and the (58,8) level for  $^7\text{LiD}$ , compared to the level (43,8) reported previously for the  $^7\text{LiH}$  case. The spectral term values for the vibrational levels lying above  $\nu = 33$  for  $^6\text{LiH}$ , and those above  $\nu = 44$  for  $^7\text{LiD}$ , occur in an irregular order. The  $\nu = 34, J = 0$  level of  $^6\text{LiH}$  and the  $\nu = 45, J = 0$  level of  $^7\text{LiD}$  lie mainly in the inner, small well. The term values for the observed rovibrational levels, for  $2 \leq \nu \leq 32, 0 \leq J \leq 11$  of  $^6\text{LiH}$  and for  $4 \leq \nu \leq 44, 0 \leq J \leq 13$  of  $^7\text{LiD}$ , in the outer ionic well are described by a set of Dunham-type coefficients. Together with previous observed term values of  $^7\text{LiH}$ , a combined isotopomer Dunham-type analysis has been performed, and five hydrogen and three lithium mass-dependent Born–Oppenheimer breakdown correction terms for the C  $^1\Sigma^+$  state are determined.

## I. Introduction

Lithium hydride, the simplest neutral heteronuclear molecule, has been the object of intensive theoretical and spectroscopic interest since the 1930s. A comprehensive and critical review for this molecule was compiled by Stwalley and Zemke.<sup>1</sup> Up to now only five electronic states X  $^1\Sigma^+$ , A  $^1\Sigma^+$ , B  $^1\Pi$ , C  $^1\Sigma^+$ , and D  $^1\Sigma^+$  have been identified by conventional spectroscopy<sup>2–7</sup> and by laser spectroscopy,<sup>8–22</sup> although some more electronic states have been predicted theoretically.<sup>23–29</sup> The four naturally occurring isotopomers  $^6\text{LiH}$ ,  $^7\text{LiH}$ ,  $^6\text{LiD}$ , and  $^7\text{LiD}$  have significantly different reduced masses, and they form an optimal system for investigating the adiabatic and nonadiabatic effects due to the breakdown of the Born–Oppenheimer approximation.<sup>1,30</sup>

Our recent spectral studies<sup>20–22</sup> were focused on the most abundant  $^7\text{LiH}$  molecule. We demonstrated that its C  $^1\Sigma^+$  state is a double-well potential,<sup>28,29</sup> with a small well at shorter internuclear distance and a broad well at longer internuclear distance, as shown in Figure 1. This is attributed to the avoided crossings between the valence and Rydberg atomic configurations and between the ionic and neutral configurations. On the other hand, we found that the observed lower part of its D  $^1\Sigma^+$  electronic state would be better characterized by a vibronic approach, due to the breakdown of the Born–Oppenheimer approximation for this electronic state.<sup>31</sup>

In this work, we have extended our observations to the C  $^1\Sigma^+$  state of  $^6\text{LiH}$  and  $^7\text{LiD}$  isotopomers, aiming (1) to confirm the double-well characteristics observed previously in the  $^7\text{LiH}$  case and (2) to investigate the effects due to the breakdown of the Born–Oppenheimer approximation. A band-resolved laser-induced fluorescence detection scheme, crucial for observing

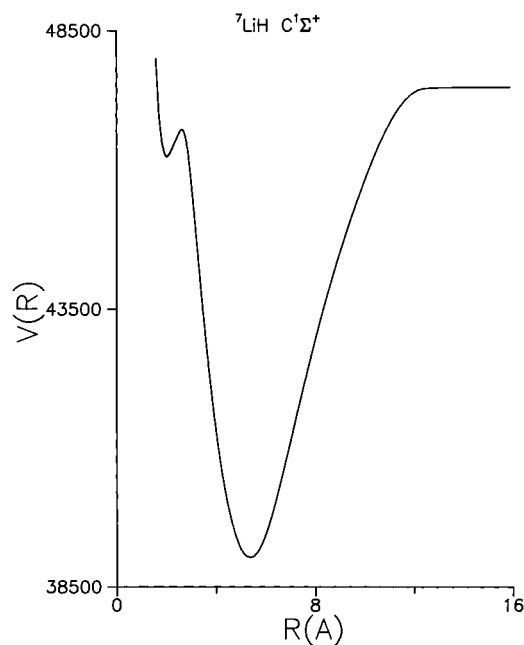


**Figure 1.** A hybrid C  $^1\Sigma^+$  potential energy curve, relative to the potential minimum of the ground electronic state (see also Figure 1 of ref 22).  $U(R)$  is in  $\text{cm}^{-1}$  and  $R$  in angstroms.

the less abundant  $^6\text{LiH}$  isotopomer, was used. Forty-two  $^6\text{LiH}$  vibrational levels and fifty-five  $^7\text{LiD}$  vibrational levels have been observed. The absolute vibrational numbering of the  $^7\text{LiD}$  C  $^1\Sigma^+$  state is identified via a comparison between observed term values and the calculated values. Spectral term values for the outer ionic well of the  $^6\text{LiH}$  C  $^1\Sigma^+$  state and for  $^7\text{LiD}$  are respectively described by a set of Dunham-type coefficients. Together with observed term values<sup>21</sup> for  $^7\text{LiH}$ , a combined isotopomer Dunham-type analysis<sup>32</sup> is performed for the three

\* To whom correspondence should be addressed. Email: wtluh@dragon.nchu.edu.tw. Fax: 886-4-2286-2547.

observed isotopomers, and the hydrogen and lithium atomic mass-dependent Born–Oppenheimer breakdown (B–O–B) correction terms for the  $C^1\Sigma^+$  state are determined.

## II. Experimental Section

The experimental setup is similar to the one used for the  $^7\text{LiH}$  isotopomer.<sup>21,22</sup> In this work, two different laser systems were used. The first laser system was composed of a frequency-doubled 10-Hz Q-switched Nd:YAG laser (Lumonics YM600), with a pulse width of 7 ns and at a pulse energy range of 20–40 mJ, and a dye laser (Lumonics HD500). The dye laser beam was frequency-doubled by a frequency-doubling system (Inrad autotracker II) to generate an ultraviolet PUMP laser beam for exciting the  $^6\text{LiH}$  (or  $^7\text{LiD}$ ) molecule from its  $X^1\Sigma^+$  state to its  $A^1\Sigma^+$  state. For covering the optimal spectral range of six  $^6\text{LiH}$  A(5–10)–X(0) bands and eight  $^7\text{LiD}$  A(5–12)–X(0) bands, the methanol solutions of two laser dyes, LDS698 and LDS722 (Exciton), were used as active media. The second laser system was composed of another frequency-doubled 10-Hz Q-switched Nd:YAG laser (Quantel BW), with a pulse width of 4 ns and at a pulse energy range of 10–30 mJ, and another dye laser (Lumonics HD500). The dye laser was used as a PROBE laser beam for probing the excited electronic state of interest. The methanol solutions of eleven laser dyes R575, R590, R610, R640, DCM, LDS698, LDS722, LDS759, LDS821, LDS867 and LDS925 were used as active media. The laser pulse energy and the laser line width were respectively 0.3–0.5 mJ and 0.1  $\text{cm}^{-1}$  for the PUMP laser, and 0.5–1.0 mJ and 0.04  $\text{cm}^{-1}$  for the PROBE laser. The laser frequencies above 14000  $\text{cm}^{-1}$  were calibrated by a reference spectrum of  $I_2$ , and those below 14000  $\text{cm}^{-1}$  were calibrated by an optogalvanic spectrum, taken either with a Ne-filled sodium/potassium hollow cathode lamp (Perkin-Elmer) or with an Ar-filled lithium hollow cathode lamp (Perkin-Elmer). The uncertainty of frequency measurements is about 0.1  $\text{cm}^{-1}$ . The PUMP laser beam and the PROBE laser beam were aligned collinearly along the axis of the longer arms of a five-arm crossed heat-pipe oven. Two digital delay/pulse generators regulated the pulse delay between the PROBE laser pulse and the PUMP laser pulse. Two different heat-pipe ovens, each containing about 10 g of naturally abundant lithium metal (STREM, 3N) in its center, were used. They were operated under 1 Torr argon and at  $\sim 950$  K. At 950 K,  $^6\text{LiH}$  and  $^7\text{LiD}$  isotopomers have maximum populations at the rotational level  $J'' = 6$  and 8, respectively; and the Doppler widths for their A–X transition lines are respectively  $\sim 0.22$  and  $\sim 0.20$   $\text{cm}^{-1}$ . For the heat-pipe oven used for the  $^7\text{LiD}$  isotopomer,  $\text{D}_2$  gas was intermittently added to keep  $^7\text{LiD}$  observable. In a natural lithium metal sample, the relative abundance<sup>33</sup> for  $^6\text{Li}$  and  $^7\text{Li}$  isotopes are respectively 7.59(4)% and 92.41(4)%. To increase spectral selectivity for observing the less abundant  $^6\text{LiH}$  isotopomer, we employed a band-resolved A–X ( $v'-v''$ ) laser-induced fluorescence detection scheme, in which a monochromator was used as a tunable band-pass filter. A photomultiplier detector detected the band-resolved fluorescence. The detected signal was fed into a boxcar-averager-gated-integrator system, and the averaged output was then recorded by a personal computer. The OODR fluorescence depletion spectrum was obtained by monitoring the variation of the band-resolved A–X fluorescence intensity as the PROBE laser was scanned, while the PUMP laser was fixed to a particular  $^6\text{LiH}$  (or  $^7\text{LiD}$ ) A–X rovibrational transition.

## III. Results and Analysis

**A. OODR Results.** The OODR spectra were taken by monitoring the band-resolved  $^6\text{LiH}$  (or  $^7\text{LiD}$ )  $A^1\Sigma^+ - X^1\Sigma^+$

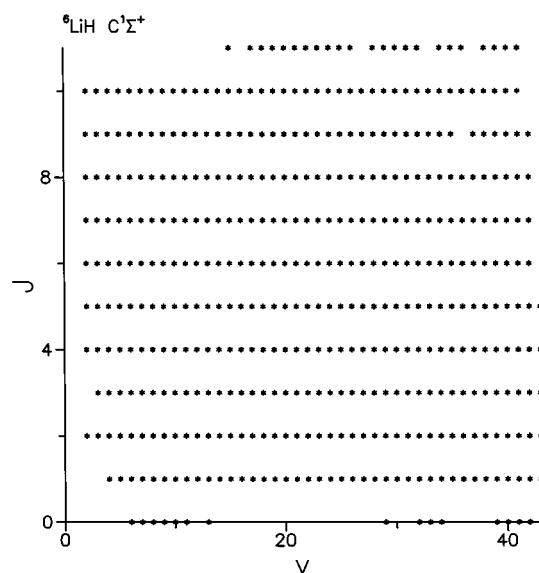


**Figure 2.** The ( $v, J$ ) data field observed. A total of 448 rovibrational levels of the  $^6\text{LiH} C^1\Sigma^+$  electronic state.

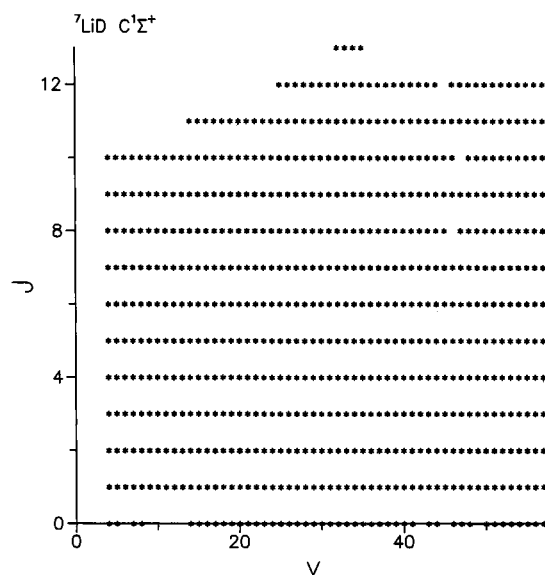


**Figure 3.** The ( $v, J$ ) data field observed. A total of 674 rovibrational levels of the  $^7\text{LiD} C^1\Sigma^+$  electronic state.

fluorescence intensity at pertinent spectral positions. The observation band-pass was set at 5 or 9 nm, depending on the monochromator used. Several rovibrational energy levels ( $v' = 5-12$ ,  $J' = 1-13$ ) of the  $A^1\Sigma^+$  state were used as intermediate states. For the  $^6\text{LiH} C^1\Sigma^+$  state, we observed a total of 720 transitions, corresponding to 448 rovibrational levels among 42 vibrational levels, which included 10 transitions observed previously for identifying absolute vibrational numbering via the isotopic shift measurements.<sup>21</sup> For the  $^7\text{LiD} C^1\Sigma^+$  state, we observed a total of 1242 transitions, corresponding to 674 rovibrational levels among 55 vibrational levels. Figures 2 and 3 present the data field observed for the two isotopomers. The lowest and highest observed vibrational levels are 2 and 43 for  $^6\text{LiH}$ , 4 and 58 for  $^7\text{LiD}$ . We could not observe the lowest two ( $v = 0-1$ ) vibrational levels of  $^6\text{LiH}$  and the lowest four ( $v = 0-3$ ) vibrational levels of  $^7\text{LiD}$  because the expected transitions, having favorable Franck–Condon factors and transition moments, lie outside the effective wavelength limit of 965 nm for the dye laser we had. Among the highest observed vibrational levels, the highest observed rovibrational levels are the (43,5)

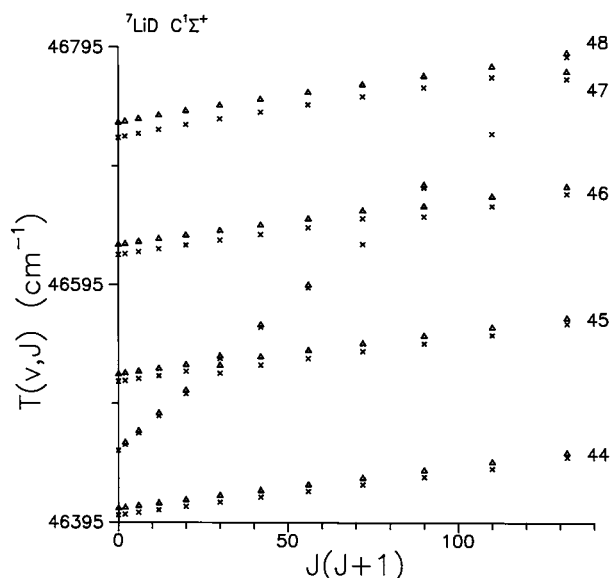


**Figure 4.** A comparison between observed term values and calculated ones. Triangle symbols denote the observed term values for the rovibrational levels of the  $\nu = 44\text{--}48$  vibrational levels of  ${}^7\text{LiD}$ , and cross symbols denote the calculated values from a hybrid potential energy curve reported previously for the  ${}^7\text{LiH}$  case.<sup>21</sup>

level for  ${}^6\text{LiH}$  and the (58,8) level for  ${}^7\text{LiD}$ , respectively, compared to the level (43,8) reported previously for the  ${}^7\text{LiH}$  case.<sup>21</sup>

The absolute vibrational quantum number of the  ${}^7\text{LiD } C^1\Sigma^+$  state is identified via a comparison between the observed term values and the respective theoretical values calculated with a hybrid potential reported previously for the  ${}^7\text{LiH}$  case.<sup>21</sup> This is demonstrated in Figure 4, which portrays observed and theoretical term values for the crucial  $\nu = 44\text{--}48$  part of the  ${}^7\text{LiD}$  potential energy curve. Note that the term value of each observed rovibrational level is obtained by adding the PROBE frequency and the term value for the intermediate rovibrational level of the A  $1\Sigma^+$  electronic state, which was calculated from Dunham-type coefficients reported by Vidal and Stwalley.<sup>34</sup>

For magnifying the peculiarity of the C  $1\Sigma^+$  excited electronic state, we present its spectral results in two different regimes, the upper irregular regime and the lower ionic well regime.

**B. The Upper Irregular Regime.** Figure 5 portrays the term values for the observed rovibrational levels of the  $\nu = 33\text{--}43$  vibrational levels of  ${}^6\text{LiH}$ , and Figure 6 for the  $\nu = 44\text{--}58$  vibrational levels of  ${}^7\text{LiD}$ . The term values in this regime are found to occur in an irregular order, particularly among the  $\nu = 34\text{--}37$  levels of  ${}^6\text{LiH}$ , and  $\nu = 45\text{--}48$  of  ${}^7\text{LiD}$ . In Figure 5 we found three switches of vibrational quantum numbers at  $J = 5, 8$  and  $10$ , and in Figure 6 three  $\nu$  switches at  $J = 5, 9$  and  $11$ . Each  $\nu$  switch can be attributed to an avoided crossing,<sup>35</sup> and such a  $\nu$  switch can be spectrally observed. Figure 7 presents two such spectra, spectrum (a) portrays the C(35,4)–A(7,5) and C(34,6)–A(7,5) transitions of  ${}^6\text{LiH}$ , and spectrum (b) the C(46,4)–A(8,5) and C(45,6)–A(8,5) transitions of  ${}^7\text{LiD}$ .

The observation of multiple  $\nu$  switches can be attributed to the existence of an inner well. A vibrational level in an inner well would have a bigger rotational constant  $B_v$ , compared to a smaller rotational constant for a vibrational level in the outer well, and this in turn would lead to multiple avoided crossings. Observed vibrational and rotational constants,  $G_v$  and  $B_v$ , for the vibrational levels  $\nu = 32\text{--}43$  of  ${}^6\text{LiH}$  are presented in Table 1, in which the observed values for  ${}^7\text{LiH}$  are also presented. The results for  $\nu = 44\text{--}58$  of  ${}^7\text{LiD}$  are presented in Table 2.

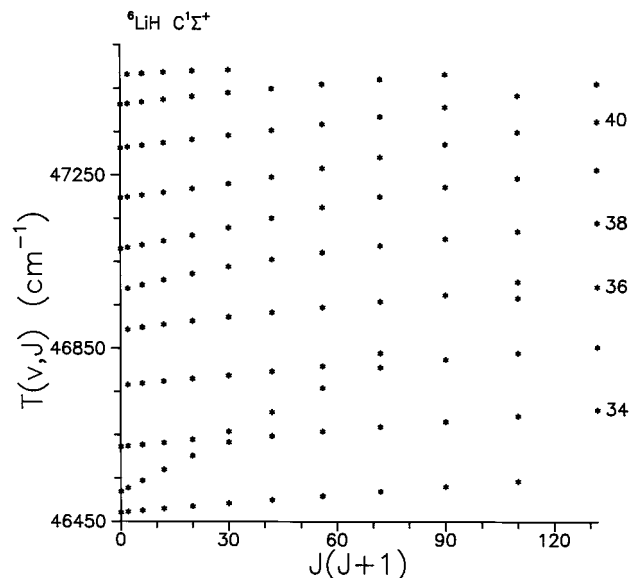


**Figure 5.** A plot of the term energies  $T(v, J)$  with respect to  $J(J+1)$  for the 117 observed rovibrational levels, among the eleven vibrational levels,  $\nu = 33\text{--}43$ , of the  ${}^6\text{LiH } C^1\Sigma^+$  electronic state. For brevity, only some even vibrational quantum numbers are designated.

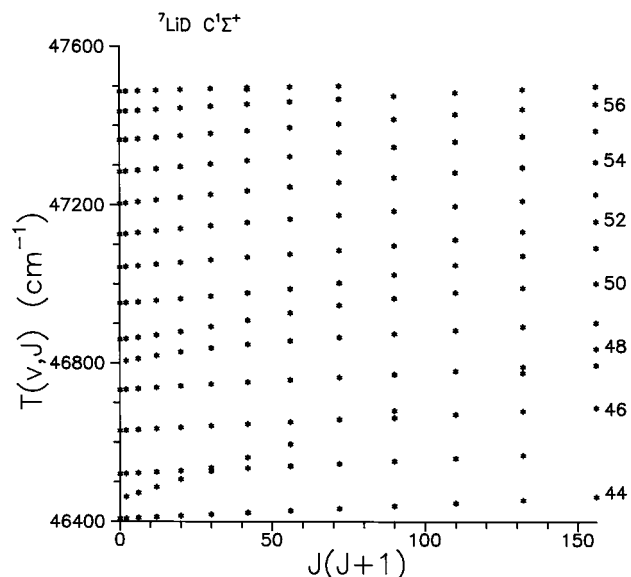


**Figure 6.** A plot of the term energies  $T(v, J)$  with respect to  $J(J+1)$  for the 187 observed rovibrational levels, among the fifteen vibrational levels,  $\nu = 44\text{--}58$ , of the  ${}^7\text{LiD } C^1\Sigma^+$  electronic state. For brevity, only some even vibrational quantum numbers are designated.

For comparison, we list also in square brackets the theoretical  $B_v$  values, which were derived from the eigenvalues for the lowest two rotational levels. The largest  $B_v$  value is found to be  $4.245$  [4.02]  $\text{cm}^{-1}$  for the  $\nu = 34$  vibrational level of  ${}^6\text{LiH}$ , and  $2.4575$  [2.44]  $\text{cm}^{-1}$  for the  $\nu = 45$  vibrational level of  ${}^7\text{LiD}$ , which are compared to the value  $3.69$  [3.85]  $\text{cm}^{-1}$  for the  $\nu = 34$  vibrational level of  ${}^7\text{LiH}$ . The  $\nu = 34$  level of  ${}^6\text{LiH}$  and the  $\nu = 45$  level of  ${}^7\text{LiD}$  are attributed to the  $\nu_{\text{in}} = 0$  level in the inner well, like the  $\nu = 34$  level<sup>21</sup> of  ${}^7\text{LiH}$ . This can be demonstrated by probability density calculations with an EIGEN program<sup>36</sup> and a  ${}^7\text{LiH}$  hybrid potential.<sup>21</sup> The probability densities for the three vibrational levels are found to concentrate mainly at internuclear distances shorter than  $2.63 \text{ \AA}$ , the location of the barrier between the inner well and the outer ionic well. The resultant probabilities are  $\sim 97\%$  for a  ${}^6\text{LiH}$  isotopomer at its (34,0) rovibrational state and  $\sim 99\%$  for  ${}^7\text{LiD}$  at (45,0), which

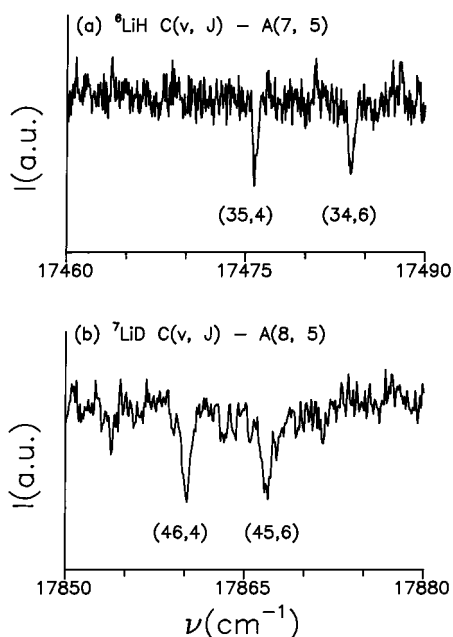


**Figure 7.** OODR fluorescence depletion spectra. Spectrum (a) portrays the OODR transitions from the intermediate A(7,5) level to the rovibrational levels (34,6) and (35,4) of the  ${}^6\text{LiH } C \ ^1\Sigma^+$  electronic state, and spectrum (b) the OODR transitions from the intermediate A(8,5) level to the rovibrational levels (45,6) and (46,4) of the  ${}^7\text{LiD } C \ ^1\Sigma^+$  electronic state.

**TABLE 1: Vibrational and Rotational Constants,  $G_v$  and  $B_v$  (in  $\text{cm}^{-1}$ ), for the Observed Upper Vibrational Levels of the  $C \ ^1\Sigma^+$  State of  ${}^6\text{LiH}$  and  ${}^7\text{LiH}$  Isotopomers**

$v$	$G_v^a$		$B_v^a$	
	${}^6\text{LiH}$	${}^7\text{LiH}$	${}^6\text{LiH}$	${}^7\text{LiH}$
32	46318.65	46266.85	0.665 [0.66]	0.655 [0.64]
33	46470.94	46420.15	0.84 [0.88]	0.65 [0.70]
34	46519.04	46517.08 <sup>b</sup>	4.245 [4.02]	3.69 [3.85]
35	46622.97	46571.91	0.735 [0.85]	0.795 [1.03]
36	46764.39 <sup>b</sup>	46714.03	0.8025 [0.89]	0.7125 [0.80]
37	46891.30 <sup>b</sup>	46846.30	1.1975 [1.26]	0.9825 [1.07]
38	46984.12	46949.965	2.05 [1.68]	1.9075 [1.59]
39	47080.05	47036.735	1.515 [1.39]	1.6675 [1.51]
40	47197.57	47149.335	1.08 [1.10]	1.075 [1.15]
41	47312.45	47265.835	1.035 [1.02]	0.995 [1.02]
42	47412.79	47372.075	0.99 [0.96]	1.025 [0.98]
43	47481.34 <sup>a</sup>	47456.58	0.5525 [0.55]	0.8925 [0.84]

<sup>a</sup>  $G_v$  is referred to the minimum of the  $X \ ^1\Sigma^+$  ground electronic state of each isotopomer, and  $B_v$  is derived from the term values for the two lowest observed rotational levels by neglecting the terms of higher order in  $J(J+1)$ . The quantities in square brackets are the theoretical  $B_v$  values calculated with a hybrid potential. <sup>b</sup> Value derived from two lowest observed rovibrational levels.

are compared to that of  $\sim 96\%$  for  ${}^7\text{LiH}$  at (34,0). The observations on the  $v = 34$  level of  ${}^6\text{LiH}$  and the  $v = 45$  level of  ${}^7\text{LiD}$  confirm again the existence of an inner well in the lithium hydride  $C \ ^1\Sigma^+$  excited electronic state.

In addition, we noted that some derived  $B_v$  values for vibrational levels around the  $v = 38$  level of  ${}^6\text{LiH}$ , around the  $v = 38$  level of  ${}^7\text{LiH}$ , and around the  $v = 49$  level of  ${}^7\text{LiD}$ , are relatively larger. The probability densities for all these vibrational states are found to be quite high at internuclear distances shorter than the barrier location. Figure 8 presents the probability densities (a) for the (38,0) rovibrational state of  ${}^6\text{LiH}$  and (b) for the (49,0) rovibrational state of  ${}^7\text{LiD}$ . The resultant probabilities for the internuclear distances shorter than the barrier location are  $\sim 59\%$  for  ${}^6\text{LiH}$  at (38,0) and  $\sim 72\%$  for  ${}^7\text{LiD}$  at (49,0), which are compared to that of  $\sim 55\%$  for  ${}^7\text{LiH}$  at (38,0).

**TABLE 2: Vibrational and Rotational Constants,  $G_v$  and  $B_v$  (in  $\text{cm}^{-1}$ ), for the Observed Upper Vibrational Levels of the  $C \ ^1\Sigma^+$  State of  ${}^7\text{LiD}$**

$v$	$G_v^a$	$B_v^a$
44	46407.30	0.345 [0.37]
45	46457.735 <sup>b</sup>	2.4575 [2.44]
46	46520.33	0.39 [0.40]
47	46629.39	0.42 [0.42]
48	46732.06	0.545 [0.60]
49	46802.815 <sup>b</sup>	1.4075 [1.23]
50	46860.01	0.815 [0.86]
51	46951.38	0.615 [0.61]
52	47042.44	0.645 [0.63]
53	47125.33	0.79 [0.69]
54	47203.26	0.875 [0.70]
55	47283.43	0.675 [0.65]
56	47363.36	0.455 [0.59]
57	47435.47	0.435 [0.52]
58	47486.41	0.305 [0.33]

<sup>a</sup> Value derived from two lowest observed rovibrational levels. <sup>b</sup>  $G_v$  is referred to the minimum of the  $X \ ^1\Sigma^+$  ground electronic state, and  $B_v$  is derived from the term values for the two lowest observed rotational levels by neglecting the terms of higher order in  $J(J+1)$ . The quantities in square brackets are the theoretical  $B_v$  values calculated with a hybrid potential.

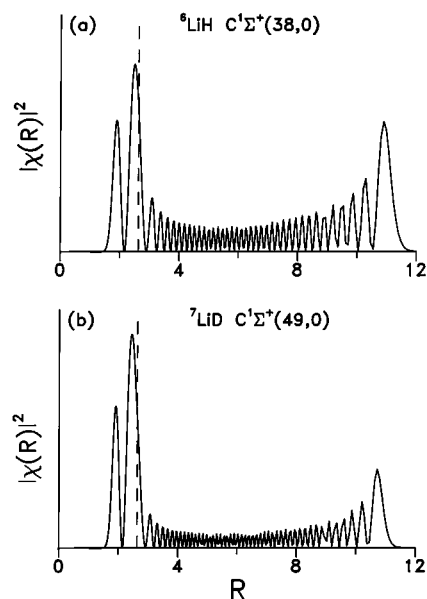


**Figure 8.** Probability densities for two rovibrational levels, (a) (38,0) of  ${}^6\text{LiH}$  and (b) (49,0) of  ${}^7\text{LiD}$ . The vertical dashed line denotes the location of the energy barrier between the inner neutral well and the outer ionic well.  $R$  is in angstroms.

Strong probabilities at short internuclear distances indicate bigger expectation values of  $1/R^2$  and in turn bigger  $B_v$  values, which are consistent with what we observed. All above spectral results for the three lithium hydride isotopomers have together demonstrated that the inner well sustains only a single vibrational level and it is indeed a small well.

**C. The Lower Ionic Well Regime.** Term values observed in this regime are found to be regular and they can be described by a set of Dunham-type coefficients. In the following, we present Dunham-type coefficients for the lower ionic regime of  ${}^6\text{LiH}$  and  ${}^7\text{LiD}$ , their RKR potential energy curves, and a combined isotopomer Dunham-type analysis with spectral data for the three isotopomers observed so far.

*C.1. Dunham-Type Coefficients.* We used two available FORTRAN programs to derive Dunham-type coefficients from spectral data. The first source code (denoted as DUN) is the



**TABLE 3: Dunham-Type Coefficients  $Y_{ij}$  and Some Spectral Parameters for the C  $^1\Sigma^+$  state of  $^6\text{LiH}$  and  $^7\text{LiD}^a$** 

	$^6\text{LiH}$	$^7\text{LiD}$
$Y_{1,0}$	298.6094 (370)	221.0111 (1300)
$Y_{2,0}$	-2.28241 (550)	-1.1045 (220)
$10^2 Y_{3,0}$	-1.420 (37)	-2.13 (19)
$10^3 Y_{4,0}$	0.6859 (110)	1.051084 (92 000)
$10^5 Y_{5,0}$	-0.768 (13)	-2.70 (25)
$10^7 Y_{6,0}$		3.9236 (360 0)
$10^9 Y_{7,0}$		-2.462 (210)
$Y_{0,1}$	0.68050 (98)	0.3670 (26)
$10^3 Y_{1,1}$	4.3 (2)	4.40 (75)
$10^4 Y_{2,1}$	-4.735 (130)	-4.544 (760)
$10^5 Y_{3,1}$	0.921 (25)	1.8276 (350 0)
$10^7 Y_{4,1}$		-3.80 (75)
$10^9 Y_{5,1}$		3.29 (60)
$10^5 Y_{0,2}$	-4.50 (35)	-1.70 (16)
$Y_{00}$	-0.521	-0.272
$T_e$	39027.66 ( $\pm 0.3$ )	39031.35 ( $\pm 0.3$ )
$D_e$	8466.16 ( $\pm 0.3$ )	8468.27 ( $\pm 0.3$ )

<sup>a</sup> All values are in  $\text{cm}^{-1}$ . For  $Y_{ij}$ , each parenthesized number represents a 95% confidence limit uncertainty in the last significant digits.

one used previously for the  $^7\text{LiH}$  case, and it was run on a personal computer equipped with Microsoft FORTRAN. The second source code is a recent DSParFit program (denoted as DSP) developed by Le Roy,<sup>37</sup> and it was run on a supercomputer (IBM SP2). The DSParFit program was developed for a combined isotopomer Dunham-type analysis and it could be run in a sequential rounding and refitting scheme<sup>38</sup> (denoted as DSP/SRR), by which we would obtain a set of rounded Dunham-type coefficients. The results from a combined isotopomer Dunham-type analysis will be presented in the third part of this section. For the first source code, observed term values were taken as input data. For the second source code, observed C–A OODR transition frequencies were directly taken as input data. The relevant band constants ( $G_v$ ,  $B_v$ ,  $D_v$ , etc.) for the intermediate vibrational levels of the A  $^1\Sigma^+$  state were also taken as input and they were generated from Dunham-type coefficients reported by Vidal and Stwalley.<sup>34</sup> Note that we retained only the transition frequencies and the term values that can be reproduced within  $0.1 \text{ cm}^{-1}$  in the fit.

For the  $^6\text{LiH}$  C  $^1\Sigma^+$  state, 453 observed transition frequencies and the resultant term values, corresponding to 322 observed rovibrational ( $0 \leq v \leq 32$ ,  $0 \leq J \leq 11$ ) levels, have been fitted with equal weights to a set of 11 parameters with the three schemes mentioned above. The overall standard errors (in  $\text{cm}^{-1}$ ) are 0.042 (DUN), 0.042 (DSP), and 0.043 (DSP/SRR), respectively.

For the  $^7\text{LiD}$  C  $^1\Sigma^+$  state, 823 observed transition frequencies and the resultant term values, corresponding to 446 observed rovibrational ( $0 \leq v \leq 44$ ,  $0 \leq J \leq 13$ ) levels, have been fitted with equal weights to a set of 15 parameters. The overall standard errors (in  $\text{cm}^{-1}$ ) are 0.041 (DUN), 0.041 (DSP), and 0.041 (DSP/SRR), respectively.

For each isotopomer, three resultant sets of Dunham-type coefficients are consistent with one another within their mutual uncertainties. The rounded Dunham-type coefficients for  $^7\text{LiH}$  and  $^7\text{LiD}$  are presented together in Table 3, in which the Dunham corrections,  $Y_{00}$ , and the electronic term differences,  $T_e$ , and the dissociation energies,  $D_e$ , are also given. The  $T_e$  and  $D_e$  quantities were derived by accounting for (a) the Dunham corrections<sup>34</sup> for the ground electronic state,  $1.010 \text{ cm}^{-1}$  for  $^6\text{LiH}$  and  $0.547 \text{ cm}^{-1}$  for  $^7\text{LiD}$ , (b) the lithium 3s electronic term,<sup>39</sup>  $27206.12 \text{ cm}^{-1}$ , and (c) the  $D_e$  values<sup>1</sup> for the ground

**TABLE 4: RKR Potential Energy Curve Derived from Dunham-Type Coefficients of the C  $^1\Sigma^+$  State of  $^6\text{LiH}^a$** 

$v$	$B_v$	$G_v + Y_{00}$	$R_{\min}$	$R_{\max}$
0	0.682532	148.21	5.0017	5.7261
1	0.685915	442.21	4.7474	6.0118
2	0.688434	731.54	4.5760	6.2197
3	0.690144	1016.14	4.4391	6.3977
4	0.691100	1295.97	4.3230	6.5595
5	0.691358	1571.01	4.2210	6.7115
6	0.690973	1841.24	4.1297	6.8571
7	0.690001	2106.66	4.0467	6.9983
8	0.688495	2367.27	3.9704	7.1365
9	0.686513	2623.09	3.8998	7.2727
10	0.684108	2874.16	3.8340	7.4075
11	0.681336	3120.49	3.7724	7.5415
12	0.678253	3362.13	3.7143	7.6751
13	0.674914	3599.13	3.6593	7.8085
14	0.671374	3831.54	3.6071	7.9420
15	0.667688	4059.41	3.5574	8.0757
16	0.663912	4282.80	3.5098	8.2098
17	0.660100	4501.77	3.4640	8.3443
18	0.656308	4716.38	3.4199	8.4793
19	0.652592	4926.70	3.3773	8.6149
20	0.649006	5132.78	3.3359	8.7511
21	0.645607	5334.68	3.2955	8.8880
22	0.642448	5532.47	3.2560	9.0257
23	0.639585	5726.19	3.2172	9.1640
24	0.637075	5915.90	3.1789	9.3031
25	0.634971	6101.63	3.1410	9.4431
26	0.633329	6283.43	3.1033	9.5839
27	0.632204	6461.33	3.0656	9.7257
28	0.631653	6635.35	3.0279	9.8685
29	0.631729	6805.51	2.9899	10.0125
30	0.632488	6971.81	2.9514	10.1578
31	0.633986	7134.24	2.9124	10.3045
32	0.636277	7292.79	2.8727	10.4530

<sup>a</sup>  $v$  is the vibrational quantum number; the rotational constant,  $B_v$ , and the corrected vibrational energy,  $G_v + Y_{00}$ , are in  $\text{cm}^{-1}$ ; inner and outer turning points,  $R_{\min}$  and  $R_{\max}$ , are in angstroms. Note that the lowest two vibrational levels of  $^6\text{LiH}$  are not observed, and the equilibrium internuclear distance,  $R_e$ , is  $5.3570 \text{ \AA}$ .

electronic state,  $20287.7 (\pm 0.3) \text{ cm}^{-1}$  for  $^6\text{LiH}$  and  $20293.5 (\pm 0.3) \text{ cm}^{-1}$  for  $^7\text{LiD}$ .

**C.2. RKR Potential Energy Curves.** The Dunham-type coefficients listed in Table 3 and the RKR1 program of Le Roy<sup>40</sup> were used to construct a RKR potential energy curve. Table 4 presents the resultant RKR potential energy curve in pairs of classical turning points for the vibrational range of  $v = 0$ –32 of the  $^6\text{LiH}$  C  $^1\Sigma^+$  state. Table 5 presents the RKR potential for the vibrational range of  $v = 0$ –44 of the  $^7\text{LiD}$  C  $^1\Sigma^+$  state. The potential minimum for  $^7\text{LiD}$  was found at a slightly longer internuclear distance. Note that we did not attempt to construct a hybrid potential for  $^7\text{LiD}$  since it would not affect the absolute vibrational numbering we made above. A direct potential fit analysis<sup>41</sup> for such a double-well potential is still a challenge to be solved.

**C.3. Combined Isotopomer Dunham-Type Analysis.** For vibration–rotation term values for multiple isotopomers of a given electronic state of a diatomic molecule AB, Le Roy<sup>32</sup> has recently developed a generalized Dunham level energy expansion:

$$E^\alpha(v, J) = \sum_{l \neq 0, m \neq 0} Y_{l,m}^\alpha (\mu_1/\mu_\alpha)^{m+1/2} (v + 1/2)^l [J(J+1)]^m + \sum_{l=0, m=0} [(\Delta M_A^\alpha / M_A^\alpha) \delta_{l,m}^A + (\Delta M_B^\alpha / M_B^\alpha) \delta_{l,m}^B] (\mu_1/\mu_\alpha)^{m+1/2} (v + 1/2)^l [J(J+1)]^m \quad (1)$$

where  $\Delta M_A^\alpha = M_A^\alpha - M^1_A$  and  $\alpha = 1$  identifies the select reference isotopomer. The Dunham-type coefficients for other

**TABLE 5: RKR Potential Energy Curve Derived from Dunham-Type Coefficients of the C  $^1\Sigma^+$  State of  $^7\text{LiD}^a$** 

$v$	$B_v$	$G_v + Y_{00}$	$R_{\min}$	$R_{\max}$
0	0.369088	109.95	5.1039	5.7289
1	0.372637	328.69	4.8726	5.9608
2	0.375431	545.05	4.7148	6.1263
3	0.377561	758.96	4.5883	6.2667
4	0.379114	970.35	4.4810	6.3935
5	0.380163	1179.17	4.3869	6.5121
6	0.380780	1385.37	4.3028	6.6252
7	0.381025	1588.94	4.2265	6.7345
8	0.380955	1789.86	4.1566	6.8411
9	0.380619	1988.13	4.0920	6.9456
10	0.380060	2183.73	4.0318	7.0486
11	0.379316	2376.68	3.9755	7.1504
12	0.378421	2566.98	3.9224	7.2513
13	0.377404	2754.65	3.8722	7.3516
14	0.376289	2939.70	3.8244	7.4514
15	0.375097	3122.14	3.7789	7.5507
16	0.373845	3302.01	3.7354	7.6498
17	0.372547	3479.31	3.6936	7.7488
18	0.371216	3654.06	3.6534	7.8476
19	0.369860	3826.30	3.6145	7.9464
20	0.368488	3996.04	3.5770	8.0453
21	0.367105	4163.30	3.5406	8.1442
22	0.365717	4328.10	3.5052	8.2434
23	0.364328	4490.48	3.4708	8.3427
24	0.362943	4650.46	3.4373	8.4423
25	0.361566	4808.05	3.4046	8.5423
26	0.360203	4963.28	3.3726	8.6425
27	0.358860	5116.18	3.3414	8.7432
28	0.357543	5266.77	3.3107	8.8442
29	0.356262	5415.07	3.2806	8.9457
30	0.355028	5561.11	3.2510	9.0477
31	0.353856	5704.91	3.2218	9.1501
32	0.352760	5846.50	3.1930	9.2530
33	0.351763	5985.89	3.1645	9.3564
34	0.350887	6123.11	3.1363	9.4603
35	0.350159	6258.17	3.1082	9.5647
36	0.349614	6391.09	3.0801	9.6696
37	0.349287	6521.87	3.0520	9.7751
38	0.349221	6650.51	3.0238	9.8810
39	0.349465	6777.02	2.9952	9.9876
40	0.350072	6901.39	2.9662	10.0947
41	0.351104	7023.58	2.9366	10.2026
42	0.352628	7143.57	2.9061	10.3112
43	0.354718	7261.32	2.8747	10.4208
44	0.357458	7376.75	2.8420	10.5314

<sup>a</sup>  $v$  is the vibrational quantum number; the rotational constant,  $B_v$ , and the corrected vibrational energy,  $G_v + Y_{00}$ , are in  $\text{cm}^{-1}$ ; inner and outer turning points,  $R_{\min}$  and  $R_{\max}$ , are in Angstroms. Note that the lowest four vibrational levels of  $^7\text{LiD}$  are not observed, and the equilibrium internuclear distance,  $R_e$ , is 5.4177 Å.

( $\alpha \neq 1$ ) isotopomers are obtained from the coefficients  $\{Y^1_{l,m}\}$ ,  $\{\delta^A_{l,m}\}$ , and  $\{\delta^B_{l,m}\}$  by the relation

$$Y^{\alpha}_{l,m} = [Y^1_{l,m} + (\Delta M^{\alpha}_A/M^{\alpha}_A)\delta^A_{l,m} + (\Delta M^{\alpha}_B/M^{\alpha}_B)\delta^B_{l,m}] (\mu_1/\mu_{\alpha})^{m+1/2} \quad (2)$$

The DSParFit program was developed to determine the generalized coefficients  $\{Y^1_{l,m}\}$ ,  $\{\delta^A_{l,m}\}$ , and  $\{\delta^B_{l,m}\}$  if pertinent term values are available from diatomic spectra. The magnitudes of the  $\{\delta^A_{l,m}\}$  and  $\{\delta^B_{l,m}\}$  coefficients reflect the relative measure of the Born–Oppenheimer breakdown energy corrections.

Observed C–A transitions were taken with equal weights to determine the generalized coefficients. For a combined analysis, relevant hydrogen and lithium atomic masses are all significant, unlike that for a single isotopomer mentioned in section C.1. To be consistent with the set of hydrogen and lithium isotopic atomic masses (see also Table 1 of ref 34) that were used to

**TABLE 6: Parameters for the C  $^1\Sigma^+$  Electronic State of LiH and LiD Obtained from a Simultaneous Fit of 1676 C–A Transitions for the Three Studied Isotopomers<sup>a</sup>**

	constant	$^7\text{LiH}$	$^6\text{LiH}$	$^7\text{LiD}$
$T_{0,0}$		39174.684 (90)		
$\delta Y_{0,0}$			−0.4609	2.5835
$Y_{1,0}$		294.6115 (860)	297.674236	221.06929
$Y_{2,0}$		−1.98711 (1900)	−2.0286401	−1.118584
$10^2 Y_{3,0}$		−4.66 (23)	−4.80685	−1.9692836
$10^3 Y_{4,0}$		3.0079 (1600)	3.1349427	0.9538788
$10^4 Y_{5,0}$		−1.000875 (60000)	−1.0539927	−0.23818647
$10^6 Y_{6,0}$		1.90 (12)	2.0216358	0.33931128
$10^8 Y_{7,0}$		−1.574 (94)	−1.692176	−0.210939
$Y_{0,1}$		0.66037 (140)	0.675683	0.371007
$10^3 Y_{1,1}$		6.60 (62)	6.7479	2.8271
$10^4 Y_{2,1}$		−8.59 (92)	−8.95281	−2.7241
$10^5 Y_{3,1}$		3.8859 (6100)	4.09213	0.92476
$10^6 Y_{4,1}$		−1.00 (18)	−1.064019	−0.178585
$10^8 Y_{5,1}$		1.214 (210)	1.30515	0.162694
$10^5 Y_{0,2}$		−4.60 (21)	−4.794	−1.459
$\delta^H_{0,0}$		5.171 (41)		
$10^2 \delta^H_{1,0}$		−3.90 (46)		
$10^3 \delta^H_{2,0}$		1.54 (13)		
$10^3 \delta^H_{0,1}$		−3.10 (95)		
$10^4 \delta^H_{1,1}$		1.80 (43)		
$\delta^{\text{Li}}_{0,0}$		2.770 (52)		
$10^2 \delta^{\text{Li}}_{0,1}$		−0.89 (18)		
$10^4 \delta^{\text{Li}}_{1,1}$		3.50 (75)		
no. of data	1676		440	806
no. of parameters	23			

<sup>a</sup> The parenthesized numbers are the 95% confidence limit uncertainties. The overall standard error is  $0.040 \text{ cm}^{-1}$

generate relevant band constants for the intermediate A  $^1\Sigma^+$  electronic state, we modified the relevant atomic masses in the code and present the results accordingly. Note that in fact we found no appreciable differences in the fitted coefficients, obtained with/without changing the relevant atomic masses in the DSParFit program, since the two set of masses are different only in the last few significant digits. A least number of B–O–B parameters required for each atom are determined in advance with two combined,  $\{^6\text{LiH}, ^7\text{LiH}\}$  and  $\{^7\text{LiH}, ^7\text{LiD}\}$ , data sets. The final combined data set includes a total of 1676 C–A transitions, 430 for  $^7\text{LiH}$ , 440 for  $^6\text{LiH}$ , and 806 for  $^7\text{LiD}$ , in which we retained only the transitions that could be reproduced within the uncertainty of  $0.1 \text{ cm}^{-1}$ . For the reference isotopomer, we have selected the most naturally abundant  $^7\text{LiH}$  isotopomer and the  $^7\text{LiD}$  isotopomer, for which we have observed most transitions. Here we present only the results that took the  $^7\text{LiH}$  isotopomer as the reference.

Table 6 presents the results from a fit of 23 parameters, which consisted of eight  $G_v$  parameters, six  $B_v$  parameters, one  $D_v$  parameter, five hydrogen mass-dependent B–O–B parameters, and three lithium mass-dependent B–O–B parameters. In the second and third columns, constants for  $^6\text{LiH}$  and  $^7\text{LiD}$  were generated from the  $^7\text{LiH}$  constants and eq 2. Note that the relevant constants for the unobserved  $^6\text{LiD}$  isotopomer could be generated similarly. In the fit, the hydrides were presented by 14 Dunham-type coefficients, not just 10 coefficients as shown in Table 3. For  $^7\text{LiD}$ , coefficients  $Y_{1-3,0}$ ,  $Y_{0,1}$ , and  $Y_{0,2}$  listed in Table 3 and Table 6 are consistent within their mutual uncertainties, but other coefficients are different from each other.

It is noted that in the combined isotopomer analysis the electronic isotope shift can be determined by the relation<sup>41</sup>

$$\delta Y^{\alpha}_{0,0} = [(\Delta M^{\alpha}_{\text{Li}}/M^{\alpha}_{\text{Li}})\delta^{\text{Li}}_{0,0} + (\Delta M^{\alpha}_{\text{H}}/M^{\alpha}_{\text{H}})\delta^{\text{H}}_{0,0}] \quad (3)$$

The fitted quantity  $\delta^A_{0,0}$  listed in Table 6 is actually a difference between the real  $\delta^A_{0,0}$  values for the C and X electronic states.

For  $^6\text{LiH}$ , the quantity  $\delta Y_{0,0}$  is a negative value,  $-0.4609\text{ cm}^{-1}$ , which is attributed to the lithium electronic isotope shift<sup>34,41</sup> occurring on replacing  $^7\text{Li}$  by  $^6\text{Li}$  in the hydride or the deuteride. This quantity also results in large positive residues,  $0.39\text{--}0.50\text{ cm}^{-1}$ , shown in the seventh column of Table 2 of ref 21. For  $^7\text{LiD}$ , the quantity  $\delta Y_{0,0}$  is a positive value,  $2.5835\text{ cm}^{-1}$ , which is attributed to the hydrogen electronic isotope shift occurring on replacing lithium hydride by lithium deuteride.

#### IV. Conclusions

In sum, the C  $^1\Sigma^+$  excited electronic states of  $^6\text{LiH}$  and  $^7\text{LiD}$  isotopomers have been studied by a pulsed optical–optical double resonance fluorescence depletion spectroscopic technique, in which a band-resolved laser-induced fluorescence detection scheme was used. Forty-two  $^6\text{LiH}$  vibrational ( $v = 2\text{--}43$ ) levels and fifty-five  $^7\text{LiD}$  vibrational ( $v = 4\text{--}58$ ) levels have been separately observed. The absolute vibrational numbering of the  $^7\text{LiD}$  C  $^1\Sigma^+$  state is identified via a comparison between observed spectral term values and those calculated with a hybrid potential energy curve reported previously for the  $^7\text{LiH}$  C  $^1\Sigma^+$  state. Among the highest observed vibrational levels, the highest observed rovibrational levels are the (43, 5) level for  $^6\text{LiH}$  and the (58, 8) level for  $^7\text{LiD}$ , respectively, compared to the level (43,8) reported previously for the  $^7\text{LiH}$  case. The spectral term values for the vibrational levels lying above  $v = 33$  for  $^6\text{LiH}$ , and those above  $v = 44$  for  $^7\text{LiD}$ , occur in an irregular order. The lowest rotational level of the  $^6\text{LiH}$   $v = 34$  level and that of the  $^7\text{LiD}$   $v = 45$  level lie mainly in the inner, small well. The spectral term values for observed rovibrational levels ( $2 \leq v \leq 32$ ,  $0 \leq J \leq 11$ ) in the outer ionic well of the  $^6\text{LiH}$  C  $^1\Sigma^+$  state, and those ( $4 \leq v \leq 44$ ,  $0 \leq J \leq 13$ ) of the  $^7\text{LiD}$  C  $^1\Sigma^+$  state, are separately described by a set of Dunham-type coefficients. Together with previous observed term values of  $^7\text{LiH}$ , a combined isotopomer Dunham-type analysis has been performed, and five hydrogen and three lithium mass-dependent Born–Oppenheimer breakdown correction terms for the C  $^1\Sigma^+$  state have been determined.

**Acknowledgment.** This work was partly supported by the National Science Council of the Republic of China under the contract no. NSC89-2113-M-005-043. The computation time was provided by the Computer Center of National Chung Hsing University. We thank Professor William C. Stwalley for critical reading and helpful suggestions, Professor Robert J. Le Roy for providing the RKR1 and DSParFit programs, and the referees for valuable comments and suggestions.

#### References and Notes

- (1) Stwalley, W. C.; Zemke, W. T. *J. Phys. Chem. Ref. Data* **1993**, *22*, 87.
- (2) Nakamura, G. *Z. Phys.* **1930**, *59*, 218.
- (3) Nakamura, G.; Shidei, T. *Jpn. J. Phys.* **1931**, *7*, 33.
- (4) Crawford, F. H.; Jorgensen, T. *Phys. Rev.* **1935**, *47*, 358; *Phys. Rev.* **1935**, *47*, 932; *Phys. Rev.* **1936**, *49*, 745.
- (5) Velasco, R. *Can. J. Phys.* **1957**, *35*, 1204.
- (6) Li, K. C.; Stwalley, W. C. *J. Mol. Spectrosc.* **1978**, *69*, 294.
- (7) Orth, F. B.; Stwalley, W. C. *J. Mol. Spectrosc.* **1979**, *76*, 17.
- (8) Wine, P. H.; Melton, L. A. *J. Chem. Phys.* **1976**, *64*, 2692.
- (9) Rafi, M.; Iqbal, Z.; Baig, M. A. *Z. Phys. A* **1983**, *312*, 357.
- (10) Dagdigian, P. J. *J. Chem. Phys.* **1976**, *64*, 2609; *J. Chem. Phys.* **1980**, *73*, 2049.
- (11) Verma, K. K.; Stwalley, W. C. *J. Chem. Phys.* **1982**, *77*, 2350.
- (12) Ennen, G.; Ottinger, Ch. *Chem. Phys. Lett.* **1975**, *36*, 16.
- (13) Ennen, G.; Fiedler, B.; Ottinger, Ch. *J. Chem. Phys.* **1981**, *75*, 59.
- (14) Chan, Y. C.; Harding, D. R.; Stwalley, W. C.; Vidal, C. R. *J. Chem. Phys.* **1986**, *85*, 2436.
- (15) Von Moers, F.; Heitz, S.; Buesener, H.; Sagner, H.; Hese, A. *Chem. Phys.* **1987**, *116*, 215.
- (16) Luh, W. T.; Kleiber, P. D.; Lyyra, A. M.; Stwalley, W. C.; Lin, K. C. *J. Mol. Spectrosc.* **1988**, *129*, 388.
- (17) Matsushima, F.; Odashima, H.; Wang, D.; Tsunekawa, S.; and Takagi, K. *Jpn. J. Appl. Phys.* **1994**, *33*, 315.
- (18) Bellini, M.; DeNatale, P.; Inguscio, M.; Varberg, T. D.; Brown, J. M. *Phys. Rev. A* **1995**, *52*, 1954.
- (19) Bouloufa, N.; Cacciani, P.; Vetter R.; Yiannopoulou, A. *J. Mol. Spectrosc.* **2000**, *202*, 37.
- (20) Lin, W. C.; Chen, J. J.; Luh, W. T. *J. Phys. Chem. A* **1997**, *101*, 6709.
- (21) Chen, J. J.; Luh, W. T.; Jeung, G.-H. *J. Chem. Phys.* **1999**, *110*, 4402.
- (22) Huang, Y. L.; Luh, W. T.; Jeung, G.-H.; Gadea, F. X. *J. Chem. Phys.* **2000**, *113*, 683.
- (23) Brown, R. E.; Shull, H. *Int. J. Quantum Chem.* **1968**, *2*, 663.
- (24) Docken, K. K.; Hinze, J. *J. Chem. Phys.* **1972**, *11*, 4928.
- (25) Yardley, R. N.; Balint-Kurti, G. G. *Mol. Phys.* **1976**, *31*, 921.
- (26) Gatti, C.; Polezzo, S.; Raimondi, M.; Simonetta, M. *Mol. Phys.* **1980**, *41*, 1259.
- (27) Sasagane, K.; Mori, K.; Ichihara, A.; Itoh, R. *J. Chem. Phys.* **1990**, *92*, 3619.
- (28) Boutalib, A.; Gadea, F. X. *J. Chem. Phys.* **1992**, *97*, 1141.
- (29) Yiannopoulou, A.; Jeung, G.-H.; Park, S. J.; Lee, H. S.; Lee, Y. S. *Phys. Rev. A* **1999**, *59*, 1178.
- (30) Uehara, H.; Ogilvie, J. F. *J. Mol. Spectrosc.* **2001**, *207*, 143.
- (31) Gemperle, F.; Gadea, F. X. *J. Chem. Phys.* **1999**, *110*, 11197; *Europhys. Lett.* **1999**, *48*, 513.
- (32) Le Roy, R. J. *J. Mol. Spectrosc.* **1999**, *194*, 189.
- (33) Rosman, K. J. R.; Taylor, P. D. P. *J. Phys. Chem. Ref. Data* **1998**, *27*, 1275.
- (34) Vidal, C. R.; Stwalley, W. C. *J. Chem. Phys.* **1982**, *77*, 883.
- (35) Tsai, C. C.; Whang, T. H.; Bahns, J. T.; Stwalley, W. C. *J. Chem. Phys.* **1993**, *99*, 8480.
- (36) Sando, K. M.; Dalgarno, A. *Mol. Phys.* **1971**, *20*, 103.
- (37) Le Roy, R. J. *DSParFit 1.0* (A Computer Program for Fitting Multi-Isotopomer Diatomic Molecular Spectra). University of Waterloo Chemical Physics Research Report No. CP-646; University of Waterloo: Waterloo, ON, Canada, 2000. The source code and manual for this program may be obtained from the WWW site <http://theochem.uwaterloo.ca/~leroy>.
- (38) Le Roy, R. J. *J. Mol. Spectrosc.* **1998**, *191*, 223.
- (39) Moore, C. E. *Atomic Energy Levels*; U. S. National Bureau of Standards, U. S. Government Printing Office: Washington, DC, 1971; Vol. 1.
- (40) Le Roy, R. J. *RKR1* (A Computer Program Implementing the First-Order RKR Method for Determining Diatom Potential Energy Curves from Spectroscopic Constants). University of Waterloo Chemical Physics Research Report No. CP-425; University of Waterloo: Waterloo, ON, Canada, 1992. The source code and manual for this program may be obtained from the WWW site <http://theochem.uwaterloo.ca/~leroy>.
- (41) Seto, J. Y.; Morbi, Z.; Charron, F.; Lee, S. K.; Bernath, P. F.; Le Roy, R. J. *J. Chem. Phys.* **1999**, *110*, 11756.